Organophosphonate Caused Cardiac Toxicity: Action Potential Dynamics in Atrial Tissue

by Csaba K. Zoltani and Steven I. Baskin

20020617 027

Army Research Laboratory

Organophosphonate Caused Cardiac Toxicity: Action Potential Dynamics in Atrial Tissue

Csaba K. Zoltani
Computational and Information Sciences Directorate, ARL

Steven I. Baskin
U.S. Army Medical Research Institute of Chemical Defense

Abstract

Highly effective treatments for the effect of organophosphonate and organophosphate (OP) nerve agents have eluded the medical community. It is known that acetylcholine overload is one of the effects of OP toxicity, but the cellular processes leading to cardiac toxicity are still incompletely understood. This study details high performance computer simulations of the electrophysiology in atrial toxicity. It shows that hyperkalemia of the tissue, one of the manifestations of OP intoxication, promotes the processes leading to reentry, a precursor of atrial fibrillation. Then, we demonstrate that changes in two of the potassium membrane currents, i_{Kr} and i_{Ks}, can modulate the reentry process. This suggests that Class III anti-arrhythmic agents that primarily block these currents in the cardiac cells are important candidates for therapeutics of OP poisoning.

Acknowledgments

INTENTIONALLY LEFT BLANK.

Contents

INTENTIONALLY LEFT BLANK.

List of Figures

List of Tables

INTENTIONALLY LEFT BLANK.

1. Introduction

Organophosphates (OP) and organophosphonates' constituents of insecticides and nerve agents, respectively, are highly toxic substances with severe cardiovascular ramification upon exposure. An estimated 95% of the contacting agent winds up within and is transported by the vasculature and is primarily deposited in tissues of the cardium. For a review of its effects, see Baskin and Whitmer [1], Roth et al. [2], and Hassler et al. [3].

Toxicity is expressed when OP binds to acetylcholinesterase (AChE), preventing hydrolysis and resulting in an accumulation of acetylcholine (ACh) in the tissue. This overload causes negative inotropy and arrhythmia not only in the atria (bradyarrhythmia), but also in the Purkinje fibers, and produces electrical conduction anomalies. In addition, the absence of cholinergic agonists increases the calcium influx and stimulates its uptake in the sarcoplasmic reticulum (SR), thereby increasing the intracellular calcium. Accompanying this process is an increase in the vagal tone that may contribute to the generation of atrial fibrillation. Cholinergic stimulation of atrial tissue reproducibly induces atrial fibrillation (AF) [4–7].

The physiological events that culminate in AF upon cholinergic stimulation are only incompletely understood. Some of the known factors ancillary to AF are

(1) non-uniform shortening of the myocardial refractory period [7],

(2) production of intra-atrial conduction delays,

(3) bradycardia that increases susceptibility to reentry,

(4) shortening of the atrial action potential duration,

(5) cholinergic stimulation may be a sine non quo for the preparation of the subtrate where atrial reentry may occur,

(6) inhomogeneous repolarization may be necessary for atrial arrhythmia, and

(7) heterogeneity of the substrate.

OP toxicity is accompanied by elevation of the concentration of $[K^+]_0$, the extracellular potassium concentration that influences the transmembrane resistance in Purkinje fibers, and $[Na^+]_0$, whose elevation mimics ischaemia. In the atria, a biphasic behavior of conduction velocity as a function of potassium concentration has been noted. Moderate elevation of extracellular potassium (up to 8 mM) increases the conduction velocity; but in the concentration range of 8–16 mM, slowdown and eventual termination of conduction has been observed. Changes in the action potential due to toxicology-caused shifts in potassium

concentration also form the basis of an updated model of soman-caused cardiac toxicity [8].

The tremendous increase in computational resources, especially parallel processing coupled with novel experimental techniques, has allowed the emergence of models of subcellular dynamics. Thus, it is possible to emulate cellular processes and study the effect of the presence of toxic agents at a fundamental level effectively and without animal experimentation.

The following sections describe a computer study of the effect of ACh overload on the electrophysiology of atrial tissue, especially the processes leading to reentry, that subsequently and usually culminate in AF, the precursor of sudden cardiac death (SCD).

2. Materials and Methods

This report details our approach to the simulation of cardiac toxicity created by the presence of OP in atrial tissue. This study especially seeks to identify conditions that promote the modulation of membrane currents that may lead to reentry, a precursor of AF and ventricular fibrillation (VF). Conversely, it seeks to answer the question of whether it is possible to identify conditions whose modulation may reverse the process and thus suggest strategies for therapies. The approach was to simulate conditions that result from OP intoxication and to see if these conditions favor reentry of the action potential.

2.1 Prior Work

Two models of AF have been advanced — the rapidly discharging focus and reentrant excitation. Here we discuss the latter, where atrial fibrillation is manifested by rapid, irregular action potential waves of variable wavelength and timing [9–11] along reentrant paths extinguishing that are also being reestablished. These irregular waves prevent the proper functioning of the atria due to the shortening of the refractory period and the loss of the normal lengthening of refractoriness when the heart slows down. The wave of excitation returns to the tissue it previously exited and reexcites it, hence the name reentry. Until quite recently, it was believed that below a certain volume of atrial tissue reentry, one of the forms of AF could not be sustained. However, the work of Wakimoto et al. [12] showed that even in murine atria, AF is inducible. The breakup of the spiral waves signals the transition from tachycardia to fibrillation.

Moe and his collaborators [13] were the first to give a mathematical description of atrial fibrillation. Several electrophysiological models of the atria, such as those of Ramirez et al. [14], Lindblad et al. [15], and Nygren et al. [16], based on the Hodgkin and Huxley formalism and patch clamp data, are now available.

These models allow *in silico*[*] studies of the effect of changes in the membrane currents caused by pathological conditions and their effect on the subsequent changes in the action potential to be studied without resort to *in vivo* experiments.

Table 1, from Koumi et al. [17], gives an indication of the effect of ACh on atrial myocytes. Significant (38%) decrease in the action potential duration was noted when 1 µM of ACh was applied to the atrial tissue. ACh also increases conductance of the tissue and especially that of the i_{Kr} channel, which occurs during myocardial ischemia.

Table 1. Effect of ACh on atrial myocytes from Koumi et al. [17].

	Resting Membrane Potential (mV)	Action Potential Amplitude (mV)	Action Potential Duration at 90% Repolarization (ms)
Control	−73.0 ± 7.2	16.8 ± 5.0	289.4 ± 23.0
1 µM ACh	−77.4 ± 6.1	−8.1 ± 4.8	112.6 ± 14.5

2.2 The Simulation Setup

For these calculations, an atrial tissue, 3 × 3 cm, and ubsequently one of 3 × 4 cm, with its electrophysiology described by the Nygren et al. [16] model, was stimulated by a pulse of 40 µA/cm² of 2 ms in duration at one edge. The presence of OPs was modeled by patches of tissue having a $[K^+]_0$ of 10.8 up to 25.0 mM instead of the ambient 5.4 mM. This expressed the observation that hyperkalemia is one manifestation of OP toxicity. In these regions, the resting membrane potential is less negative, and depends on the potassium concentration. Admittedly, this is coarse graining the problem since localized sodium and calcium concentration deviations, among other changes found in the presence of OP, are also indicators of the change of the state of the cell. For these calculations, the tissue was represented as a slab of 300 × 300 × 1 nodes and also as 300 × 400 × 1 with node spacing of 0.01 cm. The pacing used to establish the initial conditions consisted of ten 10 pulses at 300-ms intervals.

2.3 Computational Approach

The computational experiments reported were designed to establish and simulate conditions that favor the establishment of reentry in atrial tissue affected by OP.

---

[*] *In silico* refers to the modeling of living processes on the computer.

Cardiac tissue is usually modeled as a bidomain, as two interpenetrating domains representing the inside and the outside of the cell, separated by a membrane through which the current transits from one domain to the other. In each of these domains, the potential is described by

$$\nabla \cdot D_i \nabla \phi_i = \beta I_m - I_{si} \tag{1}$$

and

$$\nabla \cdot D_e \nabla \phi_e = -\beta I_m - I_{se}. \tag{2}$$

Here, the ϕ_i and ϕ_e are intracellular and interstitial potentials, D's are the diffusion tensors, and the β is the cellular surface to volume ratio. I_m is the membrane current, and I_{si} and I_{se} are the current source densities. When the diffusion tensors of the two domains are proportional to each other, as was assumed here, the bidomain equations simplify to the monodomain model. Monodomain calculations are considerably less expensive to perform than bidomain calculations. For the calculations reported here, fiber orientation (one of the diffusion matrix entries) was assumed to be uniform.

Two other sets of equations need to be solved: equations describing the gating of the ion channels and equations for the concentration changes of the ions. Generically, these may be written as follows:

$$dy/dt = (y_\infty - y)/\tau_y, \tag{3}$$

where y represents a gating variable and τ_y the time constant. In addition, the ion concentrations had to be followed. For calcium, for example, the equation is as follows:

$$d[Ca]_i / dt = -10^{-4} I_{si} + 0.07(10^{-4} - [Ca]_i). \tag{4}$$

In equation (4), the quantities in the square brackets are the ion concentrations and I_{si} represents the L-type Ca++ current. Finally, the individual membrane currents from experimental measurements are included. No-flux boundary conditions were enforced at the edge of the tissue.

The solution consists of three steps: (1) calculation of the ionic currents, I_m, (2) the determination of the transmembrane potential V_m, the difference between the intra and the interstitial potentials, and (3) the upgrading of the field potentials. In step (3) conjugate-gradient was the solution method used.

Equal grid size, 0.01 cm in both directions, was used. Some experimentation with time step size was required, but 0.001 ms yielded stable results.

The calculations were carried out with the code CardioWave on the computer assets of the Major Shared Resource Center (MSRC) at Aberdeen Proving Ground, MD.

In parallel mode, a typical run on 16 nodes on a SGI Origin 3000 required in excess of 7 hr (in non-dedicated mode) for a grid of 300×300 to simulate 300-ms real time. For a larger number of processors improvement in wall clock time was achieved, but the speedup was not absolutely linear, as seen in Figure 1.
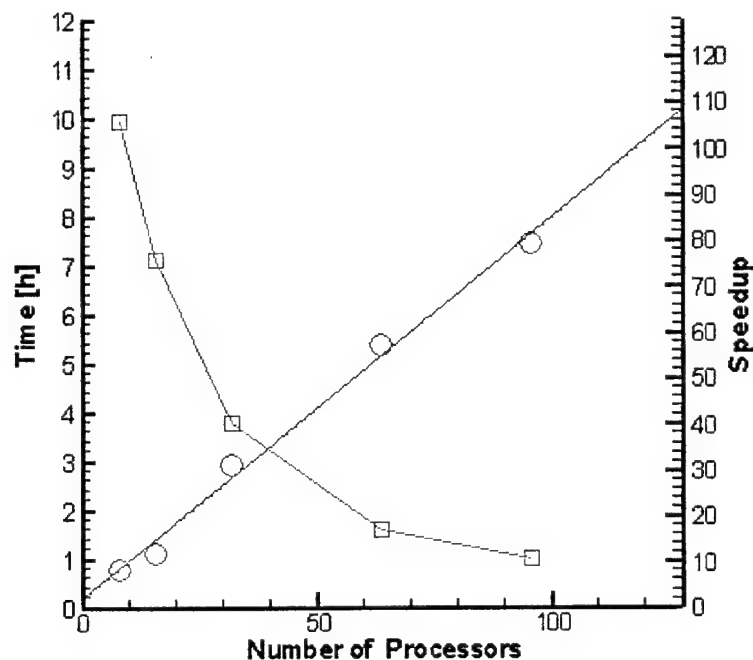
Figure 1. Performance of the code using the shared-memory Origin 3000.

3. Results

We report on three computational experiments.

(1) A pulse of 40 µA/cm² of 2 ms duration, starting at the left edge, propagates into the tissue, where it encounters two subregions of higher than normal potassium concentration. Each of these subregions was 1 cm² in size. The first was located along the central axis, flush with the left-hand boundary. The second, of the same size, was located along the lower edge of the tissue, 1 cm from the left boundary.

5

(2) The second *in silico* experiment consisted of the same tissue with one region of higher potassium concentration along the central axis of the tissue, 1 cm² in size, located at the left-hand boundary, aligned normally to the action potential advancing from the left-hand boundary.

(3) Finally, the same field of the action potential used as in (2) was examined, but with the i_{Kr} and i_{Ks} currents blocked to 99% of its nominal value. This was based on the insight that new Class III antiarrhythmic drugs, such as Azimilide, are potassium channel antagonists. Modulating these currents prolongs the duration of the action potential and the effective refractory period. It was felt that this antiarrhythmic characteristic may translate into modulating the processes that favor reentry since it is known that this drug reduces the incidence of AF and atrial flutter.

Figure 2, panels (a–d) show the encounter of the action potential, started at the left edge of the atrial tissue as it encounters a subregion with a potassium concentration, double the nominal value. This mimics cardiac toxicity caused by the presence of an OP-based substance.

In Figure 3, the action potential speeds up in the region with the higher than normal potassium concentration. The curvature in the action potential wave front is accentuated as time progresses. Behind and directly in line with the concentration, V_m, the voltage, continues to drop sharply in contrast to the adjacent areas where the drop is more gradual and in line with healthy tissue dynamics.

The front continues to distort, and aft of the heterogeneous region boundary undulations in the voltage equipotential lines appear. The front is no longer coherent, and the breakup of the integrity of the wave has commenced.

The second set of computer experiments with multiple regions of higher than normal potassium concentrations shows similar evolution of the wave. The time history of the action potential at a particular location next to the high potassium concentration mirrors the trend toward disorganization in the wave structure, signaling eventual breakup.

In the final Figure 4, the i_{Kr} and i_{Ks} currents have been reduced, mimicking the effect of antiarrhythmic drug treatment for AF. Lengthening the action potential duration (APD) is one of its effects. This effect is also apparent when contrasting Figures 3 and 4. The change in behavior is a clear indicator that the search for a therapy for OP toxicity needs to be investigated because pharmaceutics that modulate the potassium currents prolong APD, thus preventing reentry.

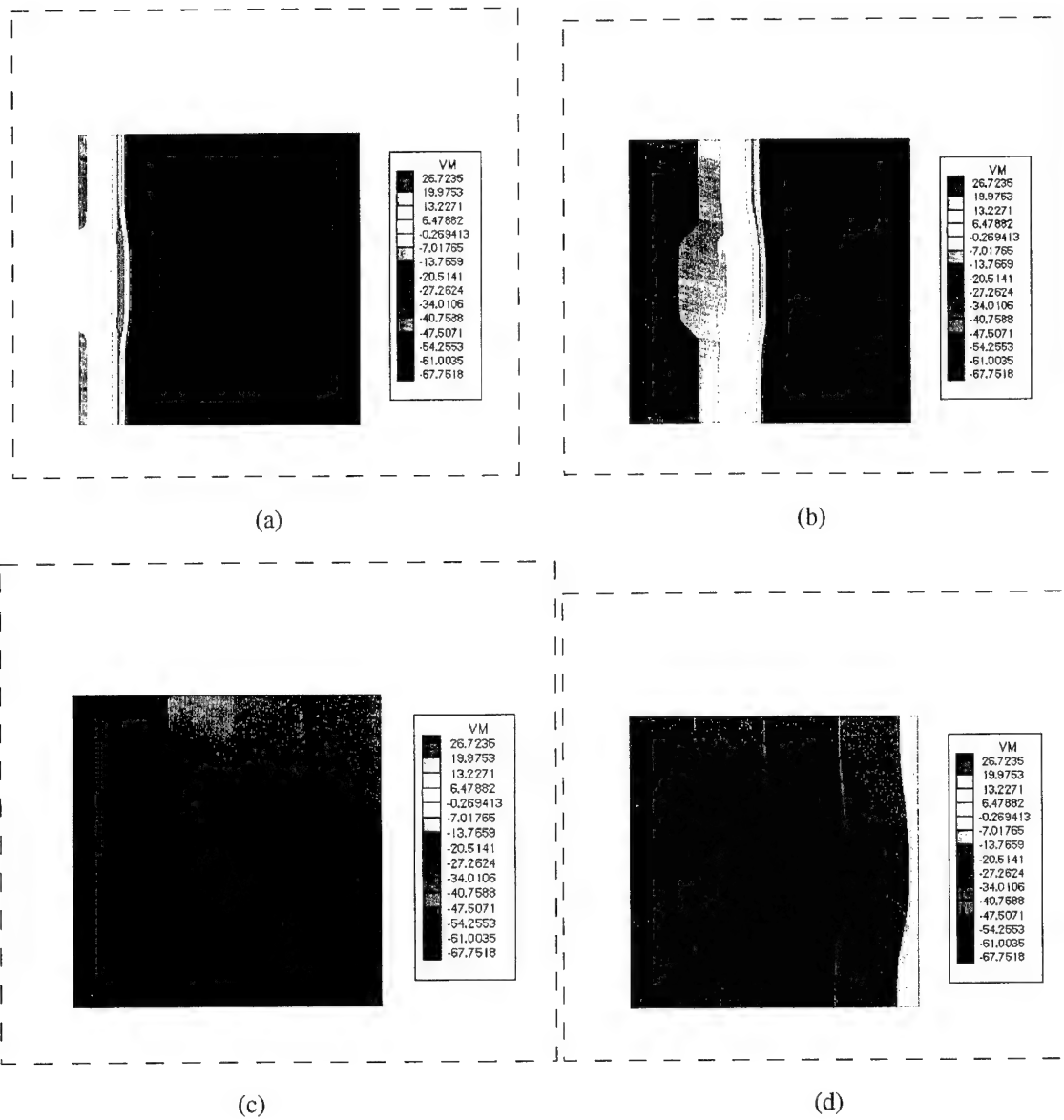Figure 2. Frame sequence showing the evolution of the action potential in atrial tissue using the Nygren model for the electrophysiology of the tissue. The times of the frames going clockwise are (a) 25 ms, (b) 60 ms, (c) 140 ms, and (d) 200 ms. The stimulus consisted of a current pulse of 40 μA/ cm² delivered to the left-most column of atrial cells. The stimulus lasted for 2 ms; VM in the legend is the voltage in mV.
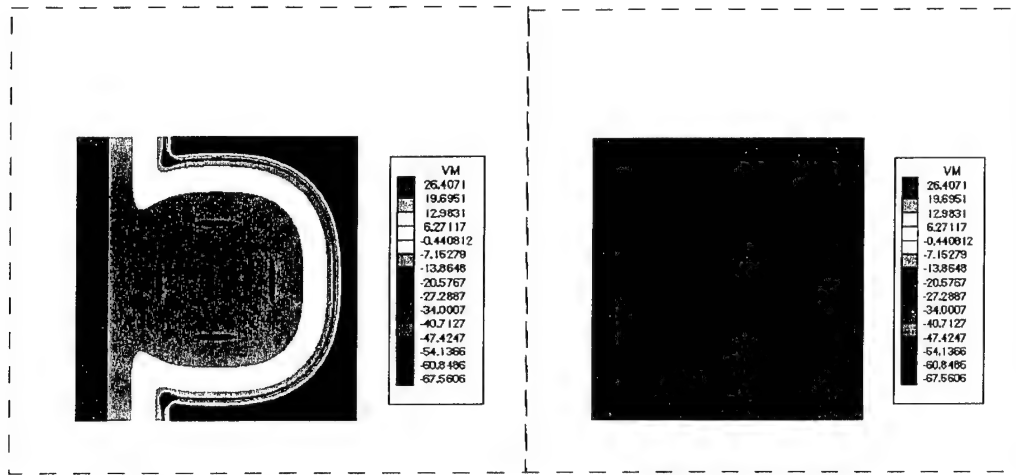
Figure 3.   The action potential in an atrial tissue containing a single hyperkalemic, cardioplegic subregion.
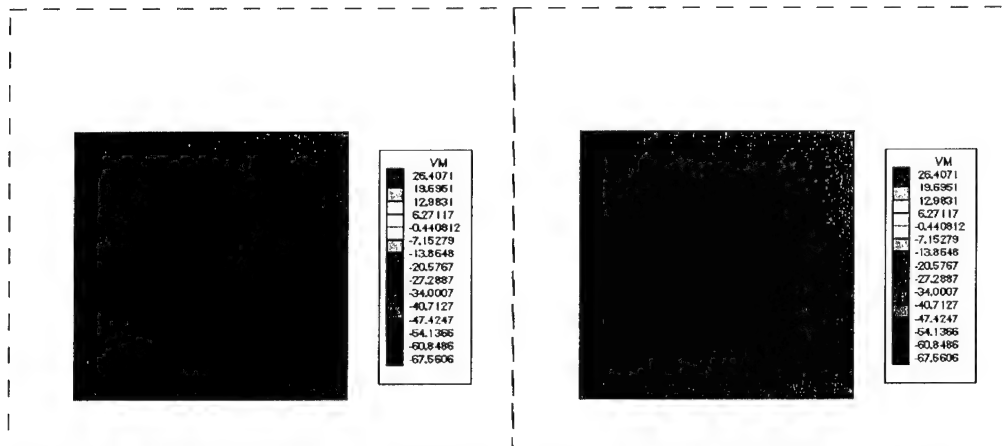
Figure 4. The effect of blocking i_{Kr} and i_{Ks} currents on the action potential.

4.   Discussion

In this study we examined the conditions, in terms of membrane currents, that promote atrial reentry, the precursor of the processes leading to AF. One of the underlying assumptions was that OP-induced ACh overload results in patches of tissue with $[K^+]_0$ in excess of normal values. When an action potential encounters such a region, processes leading to reentry are commenced. Conditions through the modulation of i_K currents were sought that could antagonize reentry. This is important, since it is believed that the morphology of AF is a progression from

8

tachycardia, through the disintegration of spiral waves in the atrial tissue, to fibrillation.

4.1 OP Toxicity Modeled as Extracellular Potassium Concentration

Changes in K^+ ion movement are central to the expression of OP-induced cardiac toxicity. An ancillary aspect is that the accumulation of K^+ ions in the interstitial space may play an important role in the overall behavior. The reasoning is as follows: excessive parasympathetic stimulation results in excessive ACh release. ACh binds to M_2 muscarinic receptors, activates the G-protein, and contributes to the hyperpolarization of the the SA node. When ACh activates $i_{K,ACh}$, K^+ exits the cell. The OP-induced ACh overload results in more receptors than usual being bound, leading also to an increase in the external concentration of potassium ions.

At high $[K^+]_0$ in the tissue, similar to the condition of ischemia or during strenuous exercise, opening less than 1% of $i_{K,ATP}$ channels causes significant shortening of AP.

Excessive concentration of potassium ions changes the concentration gradients and the response of the Na-K pump. In the initial stages of the accumulation of the potassium ions, the cells are more excitable, but as the membrane potential drops below the excitation threshold, the generation of an action potential is no longer possible. Hyperkalemia suppresses automaticity of the heart, slows conduction, and leads to bradycardia.

4.2 Reentry

It was shown that the process that can culminate in reentry in atrial tissue when a supra-threshold stimulus 40 $\mu A/cm^2$ was applied, since propagates into an OP-modified heterogeneous atrial tissue. The wave front that resulted was a spiral due to the refractory state of the tissue. Reentry is characterized by the action potential that instead of transiting and exiting the tissue, reenters previously traversed tissue.

With an ectopic beat present in the tissue, the encounter between the original stimulus and the stimulas representing the ectopic event produces a turning wave front, a precursor for reentry.

4.3 Modulation of Reentry in the Atria

Qu et al. [18] noted in their study of reentry in ventricular tissue that the condition for spiral wave breakup, and thus the condition for VF, was reached when the slope of the action potential restitution curve exceeded one. Flattening the restitution curve can exert an anti-fibrillatory effect.

9

In the atrial tissue studies reported here, i_{Kr} and i_{Ks} currents were modulated. At 1% of nominal value, considerable modulation of the action potential dynamics is observed. The block of the inward current can contribute to APD prolongation, especially at shorter cycle lengths. This suggests that Class III drugs that prolong APD have the potential for prophylaxis or treatment of OP-caused atrial arrhythmias.

4.4 Summary

Computer experiments to simulate reentry in atrial tissue with OP-induced ACh overload were performed. The presence of the OP was modeled as local potassium overload. The experiments showed the incipient processes that can enhance transition from atrial tachycardia to atrial fibrillation. It was demonstrated that modulation of membrane current affects changes in the process leading to reentry. Possible conditions for the elimination for reentry in this tissue model were found. This suggests viable new approaches to preventing and treating OP toxicity. Further computer studies and planned *in vivo* experiments at the U.S. Army Medical Research Institute of Chemical Defense (USAMRICD), Aberdeen Proving Ground, MD, in the near future should help to validate this approach.

5. References

1. Baskin, S. I., and M. P. Whitmer. "The Cardiac Toxicology of Organophosphorus Agents." *Cardiac Toxicology*, edited by S. I. Baskin, Boca Raton, FL: CRC Press, 1991.

2. Roth, A., I. Zellinger, M. Arad, and J. Atsmon. "Organophosphates and the Heart." *Chest,* vol. 103, pp. 576–582, 1993.

3. Hassler, C. R., R. R. Moutvic, D. B. Stacey, and M. P. Hagerty. "Studies of the Action of Chemical Agents on the Heart." AD–A209 219, U.S. Army Medical Research and Development Command, Fort Detrick, MD, 1988.

4. Burn, J. H., E. M. Vaughn Williams, and J. M. Walker. "Effects of Acetylcholine in Heart-Lung Preparations Including the Production of Auricular Fibrillation." *Journal of Physiology,* vol. 128, pp. 277–293, 1955.

5. Nahum, L. H., and H. E. Hoff. "Production of Auricular Fibrillation by Application of Acetyl-Beta-Methylcholine Chloride to Localized Region of the Auricular Surface." *American Journal of Physiology,* vol. 129, pp. 428–436 1940.

6. Schuessler, R. B., L. V. Rosenshtraukh, and J. P. Boineau, et al. "Spontaneous Tachyarrhythmias After Cholinergic Suppression in the Isolated Perfused Canine Right Atrium." *Circulation Research,* vol. 69, pp. 1075–1087, 1991.

7. Allessie, M., W. Lammers, J. Smeets, F. Bonke, and J. Hollen. "Total Mapping of Atrial Excitation During Acetylcholine-Induced Atrial Futter and Fibrillation in the Isolated Canine Heart." *Atrial Fibrillation,* edited by H. E. Kulbertus, J. B. Olsson, and M. Schlepper, Moldal, Sweden, 1982.

8. Zoltani, C. K., and S. I. Baskin. "Simulation of Acetylcholine Cardiac Overload Caused by Soman, a Cholinesterase Inhibitor." *Proceedings of the Computers in Cardiology 2000,* vol. 27, IEEE Press, pp. 243–246, 2000.

9. Falk, R. H. "Atrial Fibrillation." *New England Journal of Medicine,* vol. 344, pp. 1067–1078, 2001.

10. Allessie, M. A. "Reentrant Mechanisms Underlying Atrial Fibrillation." *Cardiac Electrophysiology: From Cell to Bedside,* 2nd ed., edited by D. P. Zipes, and J. Jalife, Philadelphia, PA: W. B. Saunders, pp. 562–566, 1994.

11. Scheinman, M. M. "Mechanism of Atrial Fibrillation: Is a Cure at Hand?" *Journal American College of Cardiologists,* vol. 35, pp. 1687–1692, 2000.

12. Wakimoto, H., C. T. Maguire, P. Kovoor, P. E. Hammer, J. Gehrmann, J. K. Triedman, and C. I. Berul. "Induction of Atrial Tachycardia and Fibrillation in the Mouse Heart." *Cardiovascular Research,* vol. 50, pp. 463–473, 2001.

13. Moe, G. K., W. C. Rheinboldt, and J. A. Abildskov. "A Computer Model of Atrial Fibrillation." *American Heart Journal,* vol. 67, pp. 200–220, 1964.

14. Ramirez, R. J., S. Nattel, and M. Courtemanche. "Mathematical Analysis of Canine Atrial Action Potentials: Rate, Regional Factors, and Electrical Remodeling." *American Journal of Physiology, Heart Circulation Physiology,* vol. 279, pp. H1767–H1785, 2000.

15. Lindblad, D. S., C. R. Murphey, J. W. Clark, and W. R. Giles. "A Model of the Action Potential and Underlying Membrane Currents in a Rabbit Atrial Cell." *American Journal of Physiology,* vol. 271, pp. H1666–H1696, 1996.

16. Nygren, A., C. Fiset, L. Firek, J. W. Clark, D. S. Lindblad, R. B. Clark, and W. R. Giles. "Mathematical Model of an Adult Human Atrial Cell. The Role of K^+ Currents in Repolarization." *Circulation Research,* vol. 82, pp. 63–81, 1998.

17. Koumi, S., C. E. Arentzen, C. L. Backer, and A. Wasserstrom. "Alterations in Muscarinic K^+ Channel Response to Acetylcholine and to G-Protein-Mediated Activation in Atrial Myocytes Isolated From Failing Human Hearts." *Circulation,* vol. 90, pp. 2213–2224, 1994.

18. Qu, Z., F. Xie, A. Garfinkel, and J. N. Weiss. "Origin of Spiral Wave Meander and Breakup in a Two-Dimensional Cardiac Tissue Model." *Annals of Biomedical Engineering,* vol. 28, pp. 755–771, 2000.

NO. OF COPIES	ORGANIZATION
2	DEFENSE TECHNICAL INFORMATION CENTER DTIC OCA 8725 JOHN J KINGMAN RD STE 0944 FT BELVOIR VA 22060-6218
1	HQDA DAMO FDT 400 ARMY PENTAGON WASHINGTON DC 20310-0460
1	OSD OUSD(A&T)/ODDR&E(R) DR R J TREW 3800 DEFENSE PENTAGON WASHINGTON DC 20301-3800
1	COMMANDING GENERAL US ARMY MATERIEL CMD AMCRDA TF 5001 EISENHOWER AVE ALEXANDRIA VA 22333-0001
1	INST FOR ADVNCD TCHNLGY THE UNIV OF TEXAS AT AUSTIN 3925 W BRAKER LN STE 400 AUSTIN TX 78759-5316
1	US MILITARY ACADEMY MATH SCI CTR EXCELLENCE MADN MATH THAYER HALL WEST POINT NY 10996-1786
1	DIRECTOR US ARMY RESEARCH LAB AMSRL D DR D SMITH 2800 POWDER MILL RD ADELPHI MD 20783-1197
1	DIRECTOR US ARMY RESEARCH LAB AMSRL CI AI R 2800 POWDER MILL RD ADELPHI MD 20783-1197

NO. OF COPIES	ORGANIZATION
3	DIRECTOR US ARMY RESEARCH LAB AMSRL CI LL 2800 POWDER MILL RD ADELPHI MD 20783-1197
3	DIRECTOR US ARMY RESEARCH LAB AMSRL CI IS T 2800 POWDER MILL RD ADELPHI MD 20783-1197

ABERDEEN PROVING GROUND

NO. OF COPIES	ORGANIZATION
2	DIR USARL AMSRL CI LP (BLDG 305)

NO. OF
COPIES   ORGANIZATION

ABERDEEN PROVING GROUND

3   CDR
        USAMRICD
        S BASKIN
        3100 RICKETTS PT RD
        APG MD 21010-5400

10   DIR USARL
        AMSRL CI
          N RADHAKRISHNAN
        AMSRL CI H
          C NIETUBICZ
        AMSRL CI HC
          A MARK
          M HURLEY
          D SHIRES
          R NAMBURU
          D PRESSEL
        AMSRL WM BC
          J DESPIRITO
          J SAHU
        AMSRL WT BF
          H EDGE

14

REPORT DOCUMENTATION PAGE

1. AGENCY USE ONLY (Leave blank)	2. REPORT DATE	3. REPORT TYPE AND DATES COVERED
	May 2002	Final Report, November 2000—August 2001

4. TITLE AND SUBTITLE
Organophosphonate Caused Cardiac Toxicity: Action Potential Dynamics in Atrial Tissue

5. FUNDING NUMBERS
1U590C
665803.731

6. AUTHOR(S)
Csaba K. Zoltani and Steven I. Baskin[*]

7. PERFORMING ORGANIZATION NAME(S) AND ADDRESS(ES)
U.S. Army Research Laboratory
ATTN: AMSRL-CI-HC
Aberdeen Proving Ground, MD 21005-5067

8. PERFORMING ORGANIZATION REPORT NUMBER
ARL-TR-2738

9. SPONSORING/MONITORING AGENCY NAMES(S) AND ADDRESS(ES)

10. SPONSORING/MONITORING AGENCY REPORT NUMBER

11. SUPPLEMENTARY NOTES
[*] U.S. Army Medical Research Institute of Chemical Defense, 3100 Ricketts Point Road, Aberdeen Proving Ground, MD 21010-5400

12a. DISTRIBUTION/AVAILABILITY STATEMENT
Approved for public release; distribution is unlimited.

12b. DISTRIBUTION CODE

13. ABSTRACT (Maximum 200 words)

Highly effective treatments for the effect of organophosphonate and organophosphate (OP) nerve agents have eluded the medical community. It is known that acetylcholine overload is one of the effects of OP toxicity, but the cellular processes leading to cardiac toxicity are still incompletely understood. This study details high performance computer simulations of the electrophysiology in atrial toxicity. It shows that hyperkalemia of the tissue, one of the manifestations of OP intoxication, promotes the processes leading to reentry, a recursor of atrial fibrillation. Then, we demonstrate that changes in two of the potassium membrane currents, i_{Kr} and i_{Ks}, can modulate the reentry process. This suggests that Class III anti-arrhythmic agents that primarily block these currents in the cardiac cells are important candidates for therapeutics of OP poisoning.

14. SUBJECT TERMS
cardiac toxicity, electrophysiology, cardiac cell modeling, high performance computing, parallel simulation, organophosphate poisoning

15. NUMBER OF PAGES
21

16. PRICE CODE

17. SECURITY CLASSIFICATION OF REPORT	18. SECURITY CLASSIFICATION OF THIS PAGE	19. SECURITY CLASSIFICATION OF ABSTRACT	20. LIMITATION OF ABSTRACT
UNCLASSIFIED	UNCLASSIFIED	UNCLASSIFIED	UL

INTENTIONALLY LEFT BLANK.